

Ain Shams University
Faculty of Engineering
Design and Production Engineering Dept.

# HEAT TREATMENT EFFECT ON THE CORROSION RESISTANCE OF SUPER DUPLEX STAINLESS STEEL

# A Thesis submitted in partial fulfilment of the requirements for the degree of PhD in Mechanical Engineering

By
Fady M. Moneeb Elsabbagh
B.Sc. Mechanical Engineering
2000

Supervised by
Prof. Dr. Mohamed Ahmed Taha
Dr. Rawia Mostafa Hamouda
Ain Shams University

#### **EXAMINERS COMMITTEE**

The undersigned certify that they have read and recommend to the Faculty of Engineering – Ain Shams University for accepting a thesis, entitled as "Investigation of Heat Treatment Effect on the Corrosion Resistance of Super Duplex Stainless Steel" (دراسة تأثير المعالجة الحرارية للصلب المقاوم للصدأ المزدوج البنية على مقاومة التآكل). Thesis is submitted by Fady Mohamed Moneeb El-Sabbagh, in partial fulfilment of requirement for the Doctor of Philosophy degree in Mechanical engineering.

Signature

- 1. Prof. Dr. Mohamed Ahmed Taha
  - Department of Design and Production Engineering
    Faculty of Engineering, Ain Shams University, Egypt
- 2. Prof. Dr. Heinz Palkowski

Institute of Metallurgy - Materials forming and Processing Clausthal University of Technology, Germany

3. Prof. Dr. Madiha Ahmed Shoeib

Central Metallurgical Research and Development Institute, Egypt

## **STATEMENT**

This thesis is submitted in the partial fulfilment of Doctor of Philosophy degree in Mechanical Engineering, Ain Shams University.

The author carried out the work included in this thesis, and no part of the thesis has been submitted for a degree or qualification in any other university.

Signature

Fady Mohamed Moneeb El-Sabbagh

Date:

# **ACKNOWLEDGEMENT**

I thank my country, Egypt, in which I was born, grown up and learned everything. And I wish to Egypt to restore its greatness and prosperity.

Then I thank my supervisors, Prof. Dr. Mohamed Ahmed Taha and Dr. Rawia Moustafa Hamouda for their continuous mentoring, support and teaching through long years I spent in my study.

Also, I thank all of my colleagues of Ain Shams University, specifically engineers Ahmed Safwat, Ahmed Taher, Ahmed Osama, Mohamed Taher, Ahmed Eldamalawy, and Peter Samir for their hard work in the experimental and testing parts, which was the core of this study. And I thank all the technicians (Mr. Saeed Farouk, Hesham, Husein, and Mohamed Zaky) for their great assistance and swift help in the practical works.

Then, I would like to thank associate professor Dr. Ahmed Moneeb for his major contribution in Chapter 6 and through review for the whole thesis, and associate professor Dr. Adel Elsabbagh for his effort in reviewing thesis linguistics.

Also, I would like to thank my father and mother, the dearest I have, who raised me up with all the good morals and habits, and gave me their love and help during my whole life

Finally, I thank my lovely wife Engy and charming daughters Jana and Deema for their utmost support and patience with me through the long years.

## **ABSTRACT**

Stainless steels are exposed to elevated temperatures during welding, casting or high temperature services. These high temperatures cause the precipitation of several intermetallic phases leading to the deterioration of the mechanical and corrosion resistance properties of stainless steels. Each of the austenitic, ferritic and duplex stainless steel families has certain time/temperature precipitation range, which allows specific phases to precipitate in the material structure.

In this work, intermetallics precipitation in the super duplex stainless steel UNS S32760 is studied. For comparison purposes, UNS S32760 is compared against two other types of stainless steel, UNS S42900 and UNS N08367, representatives of the ferritic and the super austenitic stainless steel families. Due to their corrosion resistance, these three stainless steel grades have wide range of applications from the food to the seawater handling industries, where high corrosion resistant alloys are needed.

The purpose of this study is to identify the interrelation between the different intermetallic precipitates and the austenitic, ferritic and duplex structures of the three stainless steel grades. Also, to estimate the impact of these intermetallic precipitates on the mechanical and corrosion resistance properties of the stainless steel grades.

For these three stainless steel grades several heat treatments are conducted by isotehrmal holding for different holiding times before quenching in water. Further testing is carried out by investigating the microstructure, XRD, SEM, hardness, microhardness, Charpy impact toughness and corrosion testing, then compared against each other and against the unheated material properties.

#### **SUMMARY**

In this study, the effect of the secondary phase precipitation on super duplex stainless steel UNS S32760 is studied. For comparison purposes, two other grades of stainless steels namely UNS S42900 and UNS N08367 are also investigated. The three stainless steel grades represent the ferritic, austenitic, and duplex (austenitic-ferritic) stainless steel families. This is to understand the interrelation between the intermetallic precipitates and the crystal structure of the stainless steel grades.

Some grades of stainless steels have a superior corrosion resistance, which qualify them to be used in seawater handling applications. Seawater is considered as one of the most corrosive fluids on earth. The super duplex and super austenitite stainless steel grades are suitable for the seawater applications, meanwhile the ferritic grade is suitable for less corrosive environment, such as in food related industires.

Unfortunately, several failures have occurred to these grades, when subjected to high temperature for prolonged periods of time, during fabrication (such as welding or casting processes) or during service at high temperatures. The reason for these failures was attributed to the precipitation of several secondary phases in the structure of the material when subjected to high temperatures for prolonged periods of time. The secondary phases have significant impact on the properties of the stainless steel, in which the corrosion resistance and material impact toughness are decreased.

This raises the need to study the relationship between the secondary precipitates and the different structures of the stainless steel materials. Also, this questions the suitability of these stainless steel grades to the severely corrosive seawater, with respect to the precipitated secondary phases in the structure.

In this study, Chapter 1 "1LITERATURE SURVEY" introduces the different families of stainless steels, the relations between the families, what are the alloying elements that drive to forming the stainless steel family, as well as the advantages and disadvantage of each family. Most of the disadvantages of the stainless steels are due to the precipitation of intermetallic phases, which drastically impact the mechanical and corrosion resistance properties of the stainless steels. This chapter illustrates the different types of intermetallic phases and the properties of each one.

Chapter 2 "PROBLEM DEFINITION AND PLAN OF WORK" presents the motive for this thesis based on previous field experiences that huge piping network had been failed due to seawater corrosion. The motive is to study the duplex stainless steel as a composite material composed of austenite and ferrite elements. This analogy was considered to study the effect of the constituent stainless steel family (i.e. austenite and ferrite) on the composite duplex stainless steel, from the toughness and corrosion perspectives. Then this chapter specifies the three stainless steel grades under study, which are UNS S32760, UNS N08367 and UNS S42900 representing the super duplex, super austenitic and ferritic stainless steel families respectively.

Chapter 3 "EXPERIMENTAL TECHNIQUES AND PROCEDURES" presents the testing plan for the stainless steel grades under study. The testing plan is briefed as identifying the incoming material, determining whether it needs for prior heat treatment (i.e. solution annealing), then isothermal heat treatment, and testing. The testing plan included optical microscopic investigation, scanning electron microscope (SEM), X-ray diffraction (XRD), microhardness, impact toughness and corrosion resistance testing.

Chapter 4 "RESULTS AND DISCUSSION (PHASE IDENTIFICATION)" presents a trial for identifying the precipitated phases, by using the test results of the optical microscopic investigation, SEM, XRD, and microhardness. This was conducted for each stainless steel grade under study.

In Chapter 5 "RESULTS AND DISCUSSION (MECHANICAL AND CORROSION)", the results of the impact toughness and corrosion testing are presented and evaluated.

Then, Chapter 6 "MODELLING OF SDSS" proposes a model for considering the duplex stainless steel as a composite material composed of austenite and ferrite elements. Such model is a new approach to correlate between the properties of the duplex stainless steel with its primary phases (i.e. austenite and ferrite).

Finally, in Chapter 7 the conclusions are derived and summarized.

## **NOMENCLATURE**

Al Aluminium C Carbon Cr Chromium

CPT Critical Pitting Potential

Cu Copper

DSS Duplex Stainless Steel

E<sub>p</sub> Pitting Potential

FSS Ferritic Stainless Steel

LOM Light Optical Microscope

MC Metal Carbide
Mn Manganese
Mo Molybdenum
N Nitrogen
Nb Niobium
Ni Nickel

PRE<sub>N</sub> Pitting Resistance Equivalent Number

ROM Rule of Mixture

S Sulphur

SASS Super Austenitic Stainless Steel
SCC Stress Corrosion Cracking
SDSS Super Duplex Stainless Steel

SDSS<sub>A</sub> Austenitic part of the Super Duplex Stainless Steel SDSS<sub>F</sub> Ferritic part of the Super Duplex Stainless Steel

Se Selenium

SEM Scanning Electron Microscope

Si Silicon

SS Stainless Steel

TEM Transmission Electron Microscope

Ti Titanium

UNS Unified Numbering System

V Vanadium W Tungsten

XRD X-Ray Diffraction
 α Alpha (Ferrite-Phase)
 δ Delta (Ferrite-Phase)

γ Gamma (Austenite-Phase)

 $\begin{array}{ccc} \chi & & Chi \\ \sigma & & Sigma \\ \epsilon & & Epsilon \\ \pi & & Pi \end{array}$ 

# **Table of Contents**

1	LITERATURE SURVEY	12
1.1	Families of Stainless Steels	12
1.2	Effects of the Composition	20
1.3	Corrosion Resistance of Stainless Steels	23
1.4	Secondary Phases Precipitation	24
2	PROBLEM DEFINITION AND PLAN OF WORK	35
2.1	Objective of this Study	35
2.2	Plan of Work	36
2.3	Motivation for this Study	36
3	EXPERIMENTAL TECHNIQUES AND PROCEDURES	45
3.1	Experimental Work on UNS S32760	46
3.2	Experimental Work on UNS N08367	48
3.3	Experimental Work on UNS S42900	51
4	RESULTS AND DISCUSSION (PHASE IDENTIFICATION)	54
4.1	Phase identification and Microhardness of UNS S32760	54
4.2	Phase identification and Microhardness of UNS N08367	65
4.3	Phase identification and Microhardness of UNS S42900	71
5	RESULTS AND DISCUSSION (MECHANICAL AND CORROSION)	77
5.1	Impact Toughness and Corrosion Results of UNS S32760	77
5.2	Impact Toughness and Corrosion Results of UNS N08367	84
5.3	Impact Toughness and Corrosion Results of UNS S42900	88
6	MODELLING OF SDSS	92
6.1	Rule of Mixture (ROM) Regarding Time-Temperature Conditions	92
6.2	Rule of Mixture Regarding the Microstructure	101
7	CONCLUSIONS	105
8	REFERENCES	107

# **Index of Figures**

Figure 1-1 Binary Fe-Cr equilibrium phase diagram [1]	13
Figure 1-2 Binary Fe-Ni equilibrium phase diagram [1]	15
Figure 1-3 Ternary Fe-Cr-Ni equilibrium phase diagram	20
Figure 1-4 Schaeffler-Delong diagram for assessment of ferrite contents and structure of stainless	
steels [1]	23
Figure 1-5 Precipitation of the σ-phase from the δ-ferrite phase [12]	27
Figure 1-6 Formation and growth of CrN and $\gamma_2$ from $\gamma$ and $\alpha/\gamma$ grains [12]	
Figure 1-7 TTP-diagram; possible precipitates in the stainless steels [15]	
Figure 1-8 TTP diagram for various precipitates appearing in duplex stainless steel. Curves indicate volume fraction of precipitates [12]	
Figure 2-1 Bottom view for leak in the fire fighting network (in the upper black circle) occurred due	
a hole in the pipe. Hole is located at 4 O'clock position and at the weld line between the pipe an	
the T-connection. The lower black circle indicates water spreading under the paint and	
accumulating underneath	37
Figure 2-2 Internal of defective UNS N08367 pipe showing corrosion in the weld area	
Figure 2-3 Effect of N on σ-phase precipitation in UNS N08367, etched with oxalic acid [18]	
Figure 2-4 Guidelines of ASTM A262 for detecting the precipitates [19], (a) Step Structure: Steps	
between grains, no ditches at grain boundaries, 500X; (b) Dual Structure: Some ditches at grain	
boundaries plus steps, but no one grain completely surrounded, 250X; (c) Ditch Structure: One	or
more grains completely surrounded by ditches, 500X; (d) Isolated Ferrite Pools: Observed in	
castings and welds. Steps between austenite matrix and ferrite pools, 250X	
Figure 2-5 Time-temperature constant hardness curve for Fe-30Cr after aging done between 430 and	
540 °C, starting hardness 195 to 205 HV.	
Figure 3-1 Plan of work	
Figure 3-2 Heat treatment points located on TTP curve of UNS N08367 [18]	50
Figure 4-1 Microstructure obtained for S32760 ingots after solution annealing, showing absence of	- 1
secondary phase precipitates and fine austenite grains	
Figure 4-2 Particles A and B in UNS S32760	
Figure 4-3 SEM shows the $\sigma$ -phase (Spectrum 3) adjacent to the $\gamma_2$ -phase (Spectrum 1) for UNS S32 heated at 950 °C for 230 s	
Figure 4-4 EDX analysis of the $\sigma$ -phase (Spectrum 3) adjacent to the $\gamma_2$ -phase (Spectrum 1) in UNS	30
S32760	56
Figure 4-5 Particle C in UNS S32760	
Figure 4-6 Particle D in UNS S32760	
Figure 4-7 Particle E in UNS S32760	
Figure 4-8 XRD for UNS S32760 heated at 860 °C for 1 min	
Figure 4-9 XRD for UNS S32760 heated at 700 °C for 4:40 min	
Figure 4-10 XRD for UNS S32760 heated at 430 °C for 67 min	
Figure 4-11 XRD for UNS S32760 heated at 350 °C for 166 min	
Figure 4-12 TTP scheme based on the microstructure and microhardness tests for UNS S32760	
Figure 4-13 Schematic diagram representing the shapes, locations, relevant sizes and conditions of	
formation on the TTP Diagram of the prominent particles in the UNS S32760	62
Figure 4-14 Microhardness rise of the particles in UNS S32760 of more than 285 HV	
Figure 4-15 Microhardness of the austenitic phase at each time-temperature condition, its trend line	
equation, maximum acceptable hardness (red line) and the time at which the trend line exceeded	1
the maximum acceptable hardness	
Figure 4-16 Microhardness of the ferritic phase of UNS S32760 at each time-temperature condition,	its
trend line equation, maximum acceptable hardness (red line) and the time at which the trend line	
exceeded the maximum acceptable hardness	04

Figure 4-17 TTP based on microhardness changes of the austenite and ferrite phases of UNS S32760	). 65
Figure 4-18 Microstructure of UNS N08367 in the as-received condition, etched using oxalic acid	
according to ASTM A262 practice A [19] for 15 s	66
Figure 4-19 Microstructure of UNS N08367 heated at 750 °C for 300 min	68
Figure 4-20 Microstructure of UNS N08367 heated at 860 °C for 70 min	68
Figure 4-21 Microstructure of UNS N08367 heated at 925°C for 300 min	68
Figure 4-22 XRD for UNS N08367 heated at 750 °C for 300 min.	69
Figure 4-23 XRD for UNS N08367 heated at 860 °C for 200 min.	69
Figure 4-24 XRD UNS N08367 heated at 925 °C for 300 min	70
Figure 4-25 XRD for UNS N08367 heated at 925 °C for 700 min.	70
Figure 4-26 Microstructure of the as-received UNS S42900	
Figure 4-27 XRD test results for UNS S42900 heated at 475 °C for 600 min	75
Figure 4-28 Microhardness test results for UNS S42900	76
Figure 5-1 Impact Toughness of isothermally heat treated, sub-sized UNS S32760	78
Figure 5-2 Polarization curves of heat treated specimens vs. the solution annealed UNS S32760	79
Figure 5-3 Trend lines of the toughness results of UNS N08367 at different temperatures	85
Figure 5-4 Trend lines of pitting corrosion test results conducted for UNS N08367	86
Figure 5-5 Impact toughness of the ferritic UNS S42900	88
Figure 5-6 Trendlines of pitting corrosion test results conducted for UNS S42900	89
Figure 5-7 Weight loss corrosion test results for the three tested stainless steel grades	89
Figure 6-1 Second degree curve fitting for a- experimental SDSS <sub>A</sub> b-SDSS <sub>A</sub> model c- Deviation in between the model and the experimental results	
Figure 6-2 Comparison between the experimental and modelled toughness test results for the austeni part of the SDSS	
Figure 6-3 Second degree curve fitting for a- experimental SDSS <sub>F</sub> b-SDSS <sub>F</sub> model	97
Figure 6-4 Comparison between the experimental and modelled toughness test results for the ferritic part of the SDSS	98
Figure 6-5 Comparison between the experimental and modelled corrosion weight loss results for the austenitic part of the SDSS	
Figure 6-6 Comparison between the experimental and modelled corrosion weight loss results for the ferritic part of the SDSS	
Figure 6-7 Phase evolution after heat treatment which should be considered in the rule of mixture:  Phases are ferrite, austenite, phase 1, phase 2, etc	101

# **Index of Tables**

Table 1-1 Chemical composition of ferritic stainless steel grades (wt.%) [2]	14
Table 1-2 Mechanical properties of ferritic stainless steel grades [2]	14
Table 1-3 Chemical composition of austenitic stainless steel grades (wt.%) [2]	15
Table 1-4 Mechanical properties of austenitic stainless steel grades [2]	
Table 1-5 Chemical composition of martensitic stainless steel grades (wt.%) [3]	
Table 1-6 Mechanical properties of martensitic stainless steel grades [3]	
Table 1-7 Chemical composition of PH stainless steel grades (wt.%) [2]	
Table 1-8 Chemical composition of duplex stainless steel grades (wt.%) [2]	
Table 1-9 Mechanical properties of duplex stainless steel grades [2]	
Table 1-10 Typical composition (in wt.%) of main alloying elements of some stainless steel grades	
Table 1-11 Precipitates in stainless steels [7] and [12]	
Table 1-12 Minimum and maximum microhardness values for some precipitates in duplex stainles	
steels [14]	
Table 2-1 Mechanical properties of several stainless steels and Ni-based alloys	
Table 2-2 Recommended welding filler metals for UNS N08367	
Table 3-1 Chemical composition of the SDSS specimens.	
Table 3-2 Heat treatment testing conditions for UNS S32760 specimens	
Table 3-3 Tested chemical composition of the SASS specimens	
Table 3-4 Heat Treatment testing conditions for UNS N08367 specimens	
Table 3-5 Etchants used in the etching of UNS N08367 specimens [31]	
Table 3-6 Chemical composition of the FSS specimens.	
Table 3-7 Heat treatment testing conditions for UNS S42900 specimens	
Table 4-1 The prominent secondary phase particles in UNS S32760 and their identification means	
Table 4-2 Microstructure of UNS N08367 at different temperatures and times, etched according to	
ASTM A262 practice A, for 15 s and all have same magnification	
Table 4-3 Chemical composition of the unknown phase	
Table 4-4 Description of the revealed secondary phases	
Table 4-5 Microstructures of UNS S42900 at different temperatures and holding times and all have	
same magnification	
Table 4-6 SEM and EDX results for UNS S42900 (heated at 475°C for 600 min) to investigate α'-	phase
	75
Table 5-1 Pitting potential and corresponding precipitates of UNS S32760	80
Table 5-2 EI curves for UNS S32760	
Table 5-3 Extrapolation calculated times vs. referenced time in Figure 3-2	85
Table 5-4 EI curves for UNS N08367	87
Table 5-5 EI curves for UNS S42900	90
Table 6-1 The experimental toughness and corrosion results of the studied materials	93
Table 6-2 Experimental versus model results for toughness of SDSS <sub>A</sub> and ROM using austenite an received FSS	d as- 94
Table 6-3 Experimental versus model results for toughness of SDSS <sub>F</sub> and ROM using ferrite and solution annealed SASS	95
Table 6-4 Experimental versus model results for corrosion of SDSS <sub>A</sub> and ROM using austenite and received FSS	d as- 99
Table 6-5 Experimental versus model results for corrosion of SDSS <sub>F</sub> and ROM using ferrite and solution annealed SASS	
Table 6-6 Modelling of SDSS <sub>A</sub> regarding microstructure	103
Table 6-7 Modelling of SDSS <sub>F</sub> regarding microstructure	

#### **CHAPTER I**

#### 1 LITERATURE SURVEY

Stainless steels are alloys exhibiting passive surface layers that can prevent substrate layers from further reaction with the environment. That passive layers are made of chromium oxide, which is formed by the reaction between oxygen in the environment and the alloying chromium in the material. The chromium content should be at least 10.5 wt.% [1]).

#### 1.1 Families of Stainless Steels

Stainless steels are commonly classified according to their crystalline structure into five families: martensitic, ferritic, austenitic, duplex (ferritic-austenitic), and precipitation-hardening stainless steels. The martensitic and ferritic stainless steels have body-centred cubic (BCC) crystal structure. However, the martensitic stainless steel has a distorted BCC structure. The austenitic family has face-centred cubic (FCC) structure. The duplex stainless steel consists of an even mixture of the austenitic and ferritic phases.

#### 1.1.1 Ferritic Stainless Steels

As per [1], the BCC ferritic stainless steels have a chromium content in the range of 10.5-30 wt.%. Some grades may contain molybdenum, silicon, aluminium, titanium, and niobium to present particular characteristics. Sulphur or Selenium may be added, as in the case of the austenitic grades, to improve machinability. The ferritic alloys are ferromagnetic. They can have good ductility and formability, but high-temperature strengths are relatively poor compared to the austenitic grades. Impact toughness is limited at low temperatures, such as -40 down to -50°C, below which the material becomes brittle as for common structural carbon steel grades.

In the Fe-Cr phase diagram shown in Figure 1-1, the ferritic steel compositions are on the right of the austenite ( $\gamma$ ) loop. Because the carbon content found in commercial steels shifts the  $\gamma$ -phase boundary to higher chromium contents, the addition of strong ferritizining elements becomes necessary in order to prevent the formation of austenite.

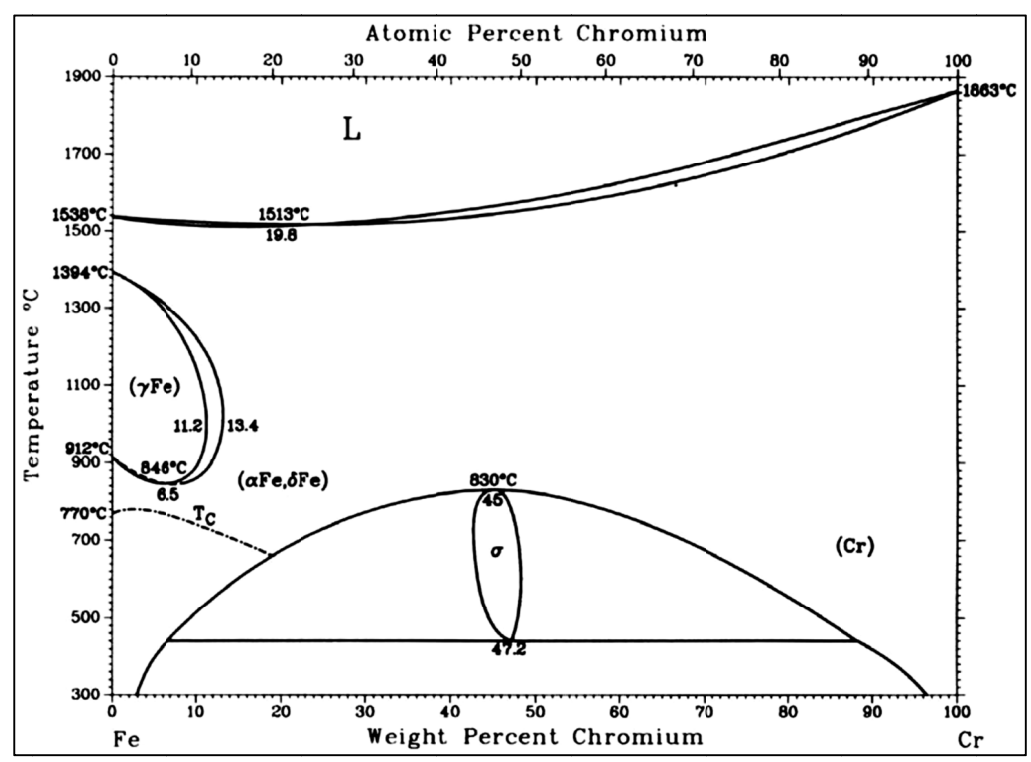


Figure 1-1 Binary Fe-Cr equilibrium phase diagram [1]

Ferritic stainless steels are designated by the AISI as 4XX series.

There are essentially three generations of ferritic stainless steels. First ferritic stainless steel generation has carbon content that is not very low, so that chromium content needs to be high. The prototype alloy is type 430 stainless steel, typically containing 0.12 wt.% maximum of carbon and 17% chromium. The second generation of ferritic stainless steels has lower carbon and low nitrogen contents, to which a stabilizer is added to tie up whatever carbon and/or nitrogen is present. The prototype of this second generation is type 409, typically 0.04C-11Cr-0.5Ti. The titanium ties up both carbon and nitrogen, leaving all of the chromium free. With titanium being ferrite stabilizer, the alloy is ferritic at all temperatures. The third generation of ferritic stainless steels has carbon and nitrogen contents of 0.02% or less, and stabilizers, such as titanium and/or niobium are often added to tie up any free interstitials. The prototype alloy is type 444 (18Cr-2Mo) [1].

The chemical compositions of the common ferritic stainless steel grades are shown in Table 1-1:

Table 1-1 Chemical composition of ferritic stainless steel grades (wt.%) [2]

UNS	Туре	C	Mn	P	S	Si	Cr	Ni	Mo	N	Others
S40500	405	0.08	1.0	0.04	0.03	1.0	11.5- 14.5	0.6	-	-	Al 0.1-0.3
S42900	429	0.12	1.0	0.04	0.03	1.0	14.0- 16.0	-	-	-	-
S43000	430	0.12	1.0	0.04	0.03	1.0	16.0- 18.0	0.75	-	-	-
S44400	444	0.025	1.0	0.04	0.03	1.0	17.5- 19.5	1.0	1.75- 2.5	0.035	Ti+Cb 0.02 + 4 (C+N) min.; 0.8 max.

Mechanical properties of the above grades are shown in Table 1-2:

Table 1-2 Mechanical properties of ferritic stainless steel grades [2]

UNS	Туре	Tensile strength, Min. (MPa)	Yield strength, Min. (MPa)	Elongation in 50mm, Min. (%)	Hardness, Max. (HBN)
S40500	405	415	170	20	179
S42900	429	450	205	22	183
S43000	430	450	205	22	183
S44400	444	690	485	15	293

#### 1.1.2 Austenitic Stainless Steels

Austenitic stainless steels have a face-centred cubic (FCC) structure that is attained through the liberal use of austenitizing elements such as nickel, manganese, and nitrogen. The most famous austenite stabilizer is nickel, see Figure 1-2. These steels are essentially nonmagnetic in the annealed condition and can be hardened only by cold working. They usually possess excellent cryogenic properties and good high-temperature strength. Their chromium content generally varies from 16 to 26 wt.%; nickel up to about 35%; and manganese up to 15% [1].

AISI designates the austenitic stainless steels stabilised with nickel as 3XX, meanwhile the manganese stabilised austenitics as 2XX. The 3XX types contain larger amounts of Ni and up to 2% of Mn, Mo, Cu, Si, Al and Ti. Nb may be added to avail characteristics such as halide (e.g. flourides and chlorides) pitting resistance and oxidation resistance. The 2XX series steels